Emergence of Koba-Nielsen-Olsen scaling in multiplicity distributions in jets produced at the LHC

G. R. Germano[*] and F. S. Navarra[†]

Instituto de Física, Universidade de São Paulo, Rua do Matão, 1371, CEP 05508-090, Cidade Universitária, São Paulo, Brazil

G. Wilk[‡]

National Centre For Nuclear Research, Pasteura 7, Warsaw 02-093, Poland

Z. Wlodarczyk[§]

Institute of Physics, Jan Kochanowski University, 25-406 Kielce, Poland

(Received 10 June 2024; accepted 17 July 2024; published 21 August 2024)

In this work we study the multiplicity distributions (MDs) of charged particles within jets in proton-proton collisions, which were measured by the ATLAS Collaboration in 2011, 2016 and 2019. The first dataset refers to jets with smaller transverse momenta ($4 < p_T < 40$ GeV) whereas the other two refer to higher p_T jets ($0.1 < p_T < 2.5$ TeV). We find that the lower p_T set shows no sign of KNO scaling and that the higher p_T sets gradually approach the scaling limit. For the lower p_T set the mean multiplicity as a function of p_T can be well-described by expressions derived from QCD with different approximation schemes. For higher (> 500 GeV) values of p_T these expressions significantly overshoot the data. We show that the behavior of the MDs can be well-represented by a sub-Poisson distribution with energy dependent parameters. In the range $40 < p_T < 100$ GeV there is a transition from sub to super Poissonian behavior and the MD evolves to a geometric distribution, which shows KNO scaling. In this way we fit the MDs in all transverse momentum intervals with one single expression. We discuss the implications of this phenomenological finding.

DOI: 10.1103/PhysRevD.110.034026

I. INTRODUCTION

Multiplicity is a global observable that allows to characterize events in all colliding systems and has been widely studied in attempts to understand multiparticle production processes. Experimentally, charged-particle multiplicity is one of the simplest observables, and its importance stretches from calibration to advanced tagging techniques. We can try to obtain the maximum information from the multiplicity distribution (MD) of charged particles to gain insights on the production mechanisms [1,2]. In high-energy proton-proton collisions, particles are produced basically in two ways. In an early stage of the collision there is a perturbative parton cascading process which is governed by the evolution equations of quantum chromodynamics (QCD). Later, the partons are converted into hadrons with additional particle production. Here the main mechanism is nonperturbative; string formation and decay. The complete description of multiparticle production is very complicated [1,2]. Nevertheless, in spite of the complexity of the subject, over the years the study of multiplicity distributions has given us valuable information about the dynamics of particle production.

One of the remarkable features exhibited by MDs is the famous Koba-Nielsen-Olsen (KNO) scaling [3–6], a phenomenon expected to be observed at asymptotically high energies. This prediction was made before the existence of QCD. Later there were several attempts to understand it in terms of quark and gluon dynamics, such as in Refs. [7,8]. In these works it was shown that KNO scaling emerges if the effective theory describing color-charge fluctuations at a scale of the order of the saturation momentum is approximately Gaussian. Moreover both nonlinear saturation effects and running-coupling evolution are required in order to obtain KNO scaling. Very recently, in Ref. [9] a MD satisfying KNO scaling was derived by solving the

[*]Contact author: guilherme.germano@usp.br
[†]Contact author: navarra@if.usp.br
[‡]Contact author: grzegorz.wilk@ncbj.gov.pl
[§]Contact author: zbigniew.wlodarczyk@ujk.edu.pl

Mueller dipole evolution equation in the double logarithm approximation. This supports the idea that gluon emission is a Markov process in which the emitted gluons are strongly ordered in rapidity.

From the experimental side there was progress too. The analysis of MDs in different systems and in different phase space regions showed that KNO scaling follows a complex pattern, appearing in certain situations and not in others. For example, in the analysis of minimum bias events in proton-proton collisions at $\sqrt{s} = 0.9$, 2.36 and 7 TeV made by the CMS Collaboration [10], KNO scaling appeared in the MD of particles in the central pseudorapidity region $|\eta| < 0.5$, whereas it was violated in the wider range $|\eta| < 2.4$. More recently, violation of KNO scaling was also observed in studies of the moments of the multiplicity distributions measured by ALICE and ATLAS data [11,12] which were found to grow with the energy [11,12].

The higher energies reached at the LHC opened new ways to study multiparticle production. Collimated groups of particles produced by the hadronization of quarks and gluons are called jets. In hadron-hadron collisions, jets are produced in high-momentum transfer scatterings. As the energy increases, we may produce jets with increasingly higher energies. These jets decay into more and more particles and they are now numerous enough so that we can study multiplicity distributions of particles produced in the jets. Multiplicity within jets is used to study both the perturbative and nonperturbative QCD processes, and since quarks and gluons have different color factors, the hadronization is sensitive to the initial parton. Thus, the particle content and its momentum distribution within jets can be used to discriminate the type of parton that initiated the jet. It is well-known that gluon-initiated jets contain larger particle multiplicities than quark-initiated jets at the same energy, and the transverse momentum of the constituent particles is harder for gluon-initiated jets [13].

The multiplicity distribution within low p_T ($4 < p_T < 40$ GeV) jets has been recently addressed in [14], where the authors presented an analysis of the ATLAS 2011 data [15,16]. They showed that they can be well-reproduced by a sub-Poissonian (SP) distribution. This finding is interesting in itself since it establishes a clear difference between the multiplicity distributions observed in minimum bias events and those observed in jets, the former being much broader than the latter. Triggering on high p_T events, such as jets, one selects perturbative QCD processes. If the QCD parton radiation would be similar to bremsstrahlung, one would expect a multiplicity distribution similar to a Poisson distribution, which is much narrower than the familiar negative binomial distribution (NBD), successful in describing minimum bias data. Surprisingly, the appropriate distribution is SP, which is still narrower. All these considerations apply to the ATLAS data which refer to transverse momenta in the range $4 < p_T < 40$ GeV.

In the theoretical analysis presented in [17,18], the authors suggested that jet multiplicity distributions follow KNO scaling if one replaces the collision energy $\sqrt{s}$ by the jet average transverse momentum p_T^{jet}. To substantiate this conjecture the authors performed a simulation with the PYTHIA-8 Monte Carlo event generator. They obtained distributions that, when plotted in the KNO style, present a very good scaling. Unfortunately, they missed the opportunity to compare the results of their simulations with the already existing data [15,19].

Empirical scaling laws *per se* are important in physics, independently of their theoretical interpretation. To study them we first have to analyze the data choosing the most relevant variables and the best way to plot them. Then we fit these data with expressions which contain some physical meaning, such as, in the present context, the negative binomial distribution. The observation of scaling and the behavior of the fitting distributions can give insights on the production dynamics and serve as a guide to theoretical microscopic studies.

In this work we will first revisit the ATLAS data and check whether they satisfy KNO scaling and also whether the average multiplicities are well described by QCD predictions. Then we will fit all the ATLAS data with a sub-Poisson distribution and analyze the energy dependence of the parameters. As it will be seen, the data suggest that the MD undergoes a transition from sub- to super-Poissonian behavior and starts to approach the KNO scaling limit.

II. REVISITING THE ATLAS DATA

In this section we perform a quite simple and model-independent exercise to check whether the existing ATLAS data [15,19] satisfy the scaling found in [17,18]. In Fig. 1 we plot the ATLAS data on jet multiplicities in the KNO form. In Figs. 1(a) and 1(b) we show the data from Ref. [15] on lower p_T jets. The two sets refer to two values of the jet R variable. We clearly see that the data violate KNO scaling. However, if we consider the higher p_T jets measured in Ref. [19] we observe the onset of scaling, as shown in Fig. 1(c), specially at $p_T > 300$ GeV. This change of behavior can be more clearly seen if we plot the ratio between the variance and the average multiplicity $[\text{Var}(n)/\bar{n}]$ which is equal to one for a Poisson distribution. In Fig. 2 we can see that this ratio is below one for lower $\bar{n}$ [Fig. 2(a)] and for lower p_T [Fig. 2(b)] and around $\bar{n} \simeq 10$ or $p_T \simeq 30$ GeV there is a clear change. The ratio becomes larger than one and we go from a sub-Poissonian to a super-Poissonian distribution. It is tempting to associate this broadening of the multiplicity distribution with the transition from quark to gluon initiated jets. In Ref. [13] the properties of quark and gluon jets were studied. In particular, it was found that the dispersion D of the multiplicity distribution from jets was $D_g \simeq 4.37$ and $D_q \simeq 4.30$ for gluon and quark jets respectively. The errors

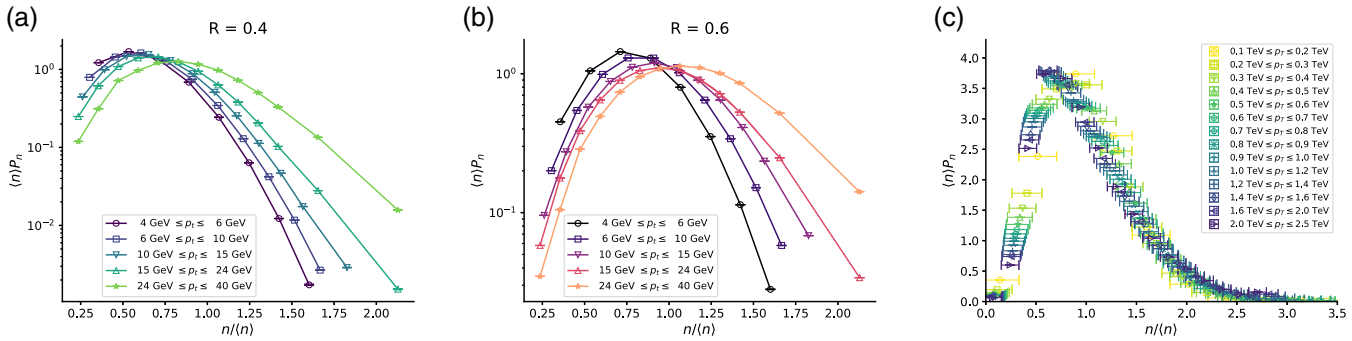

FIG. 1. Data from Ref. [15] plotted in the KNO form for (a) $R = 0.4$, (b) $R = 0.6$. c). Data from Ref. [19].

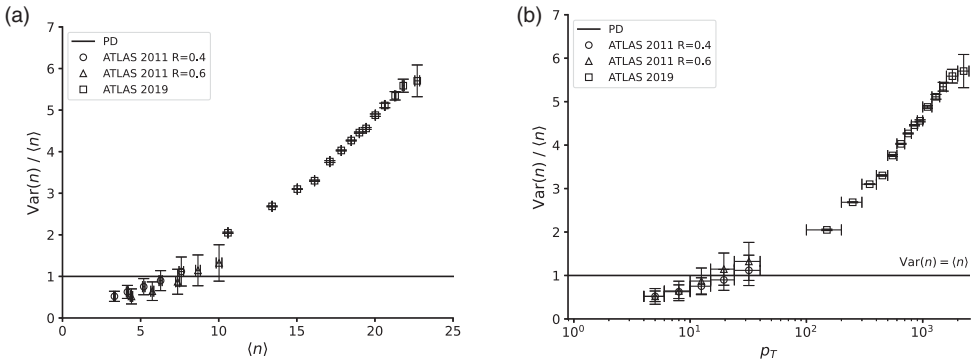

FIG. 2. Variance as a function of (a) $\bar{n}$ and (b) p_T. Data are from Refs. [15,19]. The solid line shows the result obtained with the Poisson distribution.

quoted in [13] are very large but these numbers suggest that gluon jets are broader than quark ones and the onset of the dominance of the former could be the dynamical cause of the behavior observed in Fig. 2.

From the low p_T data [15] we have extracted the average multiplicities for the $R = 0.4$ and $R = 0.6$ sets. For the higher p_T sets the average multiplicities were already given in [19] and [20]. From the theoretical point of view, the definition of the multiplicity in a jet can be rather tricky. The total hadronic multiplicity within a jet can be obtained from the jet fragmentation function and it was studied in perturbative QCD in several works [21–26]. Very recently these calculations have been done with higher precision (see Ref. [27] for a recent review of the literature). Here, for simplicity, we shall use the analytical formulas derived from perturbative QCD in the next-to-leading-logarithmic approximation (NLLA) [22] and also, more recently, in the next-to-modified-leading-log approximation (NMLLA) including next-to-leading-order (NLO) corrections to the α_s strong coupling [26]. These expressions were successfully applied to fit the multiplicities measured in e^+e^- collisions [28]. The NLLA expression is given by [22]

$$\bar{n}_{ch} = a[\alpha_s(p_T)]^b e^{c/\sqrt{\alpha_s(p_T)}}\left[1 + d\sqrt{\alpha_s(p_T)}\right], \quad (1)$$

where [22]

$$b = \frac{1}{4} + \frac{10}{27}\frac{N_f}{\beta_0} = 0.49 \qquad c = \frac{\sqrt{96\pi}}{\beta_0} = 2.27$$

$$\alpha_s(Q^2) = \frac{4\pi}{\beta_0 \ln(Q^2/\Lambda^2)} - \frac{\beta_1 \ln\ln(Q^2/\Lambda^2)}{\beta_0^3 \ln^2(Q^2/\Lambda^2)}$$

with $\beta_0 = 11 - 2/3N_f$, $\beta_1 = 102 - 38/3N_f$ and $\Lambda = 0.15$ GeV. The NMLLA-NLO expression reads [26],

$$\bar{n}_{\rm ch} = \mathcal{K}_{\rm ch} \exp\left[2.50217\sqrt{Y} - 0.491546 \ln Y - (0.06889 - 0.41151 \ln Y)\frac{1}{\sqrt{Y}} + (0.00068 - 0.161658 \ln Y)\frac{1}{Y}\right], \quad (2)$$

where

$$Y = \ln(p_T/\Lambda_{\rm QCD}).$$

In the above expressions all the parameters have already been fixed so as to reproduce the multiplicity distributions measured in e^+e^- collisions at LEP and at energies ranging

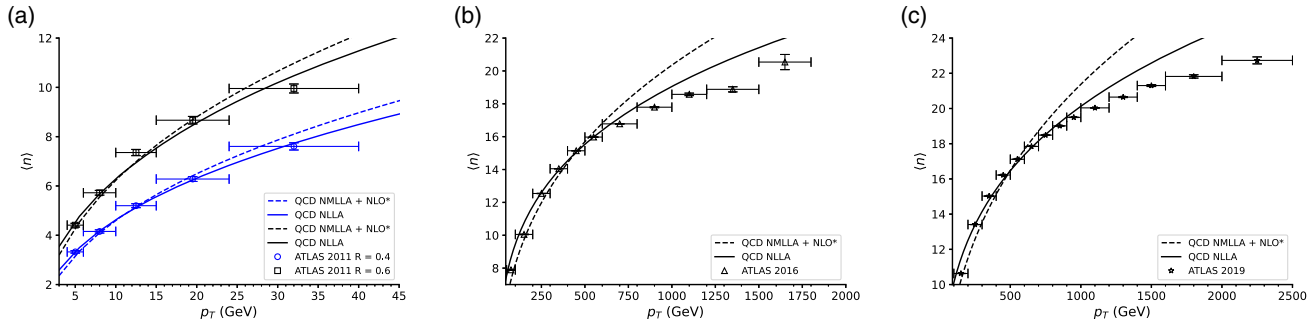

FIG. 3. Average multiplicities (data points) obtained from ATLAS, in (a) Ref. [15], (b) Ref. [20] and (c) Ref. [19]. The curves show the fits with the theoretical expressions Eq. (1) (solid line) and Eq. (2) (dashed line).

from 2 GeV $< \sqrt{s} <$ 200 GeV. In (1) the normalization a and the (higher order corrections) parameter d were adjusted. In (2) the normalization $\mathcal{K}_{\rm ch}$ and $\Lambda_{\rm QCD}$ were adjusted. Both expressions were able to yield very good fits. We assume that each of the two jets in e^+e^- collisions is initiated by one highly energetic parton, in the same way as the jets observed in pp collisions. Therefore, apart from a normalization factor, the formulas (1) and (2) can be applied to the average multiplicities studied in this work.

In Fig. 3 we show the average multiplicities. As it can be seen, the low p_T data from Ref. [15] in Fig. 3(a) are well reproduced both by (1) and (2). The parameters obtained from the fits are shown in Table I. In comparison to the jets measured in e^+e^-, both the normalization factor and $\Lambda_{\rm QCD}$ are systematically smaller. These expressions work well for the higher p_T sets from Ref. [20] shown in Fig. 3(b) and also from Ref. [19] shown in Fig. 3(c) up to $p_T \simeq$ 500–600 GeV. Up to this point, Eq. (1) and Eq. (2) seem to capture the energy dependence of the data very well. Beyond this point, they overshoot the data. In this region it is possible that gluon recombination (not yet included in the calculations) starts to play a role. In fact $gg \to g$ would reduce the number of produced partons (and hadrons). Qualitatively this effect would go in the right direction to reproduce the data.

III. THE SUB-POISSONIAN DISTRIBUTION

A sub-Poissonian distribution (SPD) is a probability distribution that has a smaller variance than the Poisson one with the same mean. A distribution which has a larger variance is called super-Poissonian and to this class belongs also the widely used negative binomial distribution (NBD). In [29,30] the SPD was introduced in the context of particle physics and applied to study MDs measured at lower energies.

Since the SPD has not been used very often, it is worth saying a few words about its origin and meaning. In particular, we would like to show how it can be obtained from a stochastic Markov process with multiplicity-dependent birth and death rates.

Let $P(n,t)$ be the probability of having n particles at time t and let us consider a very general birth-death process given by the following equations:

$$\frac{dP(0,t)}{dt} = -\lambda_0 P(0,t) + \mu_1 P(1,t), \tag{3}$$

$$\frac{dP(n,t)}{dt} = -(\lambda_n + \mu_n)P(n,t) + \lambda_{n-1}P(n-1,t) + \mu_{n+1}P(n+1,t), \tag{4}$$

where λ_n and μ_n are the birth and death rates when the multiplicity is n. Let us further assume that,

$$\lambda_n = \lambda(n+1)^{-\delta} + \sigma \quad \text{and} \quad \mu_n = n\mu. \tag{5}$$

Then, in the steady state, when $\frac{dP(n,t)}{dt} = 0$, Eq. (4) yields,

$$-[\lambda(n+1)^{-\delta} + \sigma + n\mu]P(n) + (\lambda n^{-\delta} + \sigma)P(n-1) + (n+1)\mu P(n+1) = 0. \tag{6}$$

TABLE I. Fitted values of $\mathcal{K}_{\rm ch}$ and $\Lambda_{\rm QCD}$ in Eq. (2) and values of a and d in Eq. (1) for all datasets and the corresponding values of these parameters obtained from e^+e^- collisions in [26] and [28].

	ATLAS 2011 $R = 0.4$	ATLAS 2011 $R = 0.6$	ATLAS 2016	ATLAS 2019	e^+e^-
$\mathcal{K}_{\rm ch}$	0.04(1)	0.06(3)	0.03(2)	0.03(1)	0.117(1)
$\Lambda_{\rm QCD}$ (GeV)	0.15(8)	0.15(12)	0.15(22)	0.15(19)	0.191(13)
a	0.042(5)	0.05(2)	−0.012(9)	−0.015(7)	0.53(6)
d	0.9(4)	1.1(1.4)	−13(8)	−11(4)	1.11(39)

Introducing the notation,

$$\frac{\lambda}{\mu}=\alpha \quad \text{and} \quad \frac{\sigma}{\mu}=\alpha_0, \tag{7}$$

Eq. (6) can be rewritten as

$$-[\alpha(n+1)^{-\delta}+\alpha_0+n]P(n)+[\alpha n^{-\delta}+\alpha_0]P(n-1) + (n+1)P(n+1)=0, \tag{8}$$

which yields the following recurrence relation,

$$(n+1)P(n+1)=[\alpha(n+1)^{-\delta}+\alpha_0]P(n)=g(n)P(n), \tag{9}$$

where $g(n)=(n+1)P(n+1)/P(n)=\alpha(n+1)^{-\delta}+\alpha_0$. Knowing $P(0)$, with the above expression we can construct the multiplicity distribution,

$$P(n)=\frac{P(0)}{n!}\prod_{i=0}^{n-1} g(i)=\frac{P(0)}{n!}\prod_{i=0}^{n-1}[\alpha(i+1)^{-\delta}+\alpha_0]. \tag{10}$$

Choosing $\alpha_0>0$ and $\delta=-1$ we obtain the negative binomial distribution,

$$P(n)=\frac{\Gamma(n+k)}{\Gamma(n+1)\Gamma(k)}\alpha^n(1-\alpha)^k. \tag{11}$$

where $k=1+\alpha_0/\alpha$. In the particular case when $\alpha_0=0$, the parameter $k=1$ and the above expression reduces to the geometric (Bose-Einstein) distribution,

$$P(n)=\alpha^n(1-\alpha). \tag{12}$$

Setting $\delta=0$ in (10) we obtain the Poisson distribution,

$$P(n)=\frac{\alpha^n}{n!}\exp(-\alpha). \tag{13}$$

For $\delta>0$ we get the sub-Poissonian distribution,

$$P(n)=c\frac{\alpha^n}{(n!)^{1+\delta}}, \tag{14}$$

where c is a normalization factor. Notice that when $\delta=-1$ the above expression becomes (12) apart from a constant factor.

IV. FROM SUB-POISSON TO NEGATIVE BINOMIAL DISTRIBUTION

In this section we shall use the form (14) to study the ATLAS data on multiplicity distributions in jets. We will extend the work [14] and fit all the ATLAS data from Ref. [15] and also from Ref. [19]. We will fix α and δ adjusting (14) to the data. The normalization factor c is given in terms of α and δ as

$$c=\left(\sum_1^{N_{\max}}\frac{\alpha^n}{(n!)^{1+\delta}}\right)^{-1} \tag{15}$$

where the $N_{\max}$ is the number of data points. The results are shown in Figs. 4(a) and 4(b). As it can be seen, the SPD can reproduce very well the low-p_T ATLAS data. The fitted parameters α and δ are shown in the Tables II and III, as well as the χ^2 of the fits, which is always below 2.1. Because of the discrepancies in the large n region, the χ^2 of the high p_T fits is unreasonably large and we do not show it in Table IV. As seen in Tables II–IV, for higher values of p_T the δ parameter becomes negative, which signals the transition from sub-PD to super-PD, best visible in Fig. 4(c). Notice that the simple formula (14) used here (with the parameter δ describing the departure from PD towards sub-PD or super-PD) approaches the NBD limit (where $\delta=-1$). In Fig. 4(d) we show lines obtained with the NBD written in a form slightly different from (11) and more convenient for our purposes. From (11) it is easy to see that $\bar{n}=k\alpha/(1-\alpha)$ and hence $\alpha^n(1-\alpha)^k=(\bar{n}^n k^k)/(\bar{n}+k)^{(n+k)}$. Then (11) can be rewritten as

$$P(n)=\frac{\Gamma(k+n)}{\Gamma(k)\Gamma(n+1)}\frac{\bar{n}^n k^k}{(\bar{n}+k)^{n+k}}. \tag{16}$$

The fits are very good. They show that k decreases with the jet p_T in the same way as it decreases with the energy in NBD fits of the minimum bias multiplicity distributions [11]. They also show that $\bar{n}/k$ increases with p_T indicating the approach to KNO scaling, which is reached when $\bar{n}\gg k$. Indeed, for KNO scaling, we expect the moments of the $P(z=n/\bar{n})$ distribution to be independent of $\bar{n}$. In the case of the NBD distribution, the second central moment of the $P(z)$ distribution is

$$\mathrm{Var}(z)=\frac{\mathrm{Var}(n)}{\bar{n}^2}=\frac{1}{\bar{n}}+\frac{1}{k}. \tag{17}$$

For $\bar{n}\gg k$ we have an approximate scaling. In fact, it was shown in [7] that when this ratio reaches 6 one already has a very good scaling. From the last entries of Table V we have ratios close to this number.

To summarize, we observe a transition from the low p_T region, where there is no KNO scaling, to the high p_T region, where we find the scaling shown in Fig. 1(c). In our description this is related to the fact that the SPD given by (14) turns into a super-Poisson distribution for large p_T because δ becomes negative. In turn, the super-PD distribution transforms for $\delta=-1$ into the geometric distribution (12), i.e. the NBD with $k=1$, for which we have KNO scaling. Therefore, what we observe represents a gradual change in dynamics causing the gradual (with increasing p_T) emergence of KNO scaling. Multiplicity

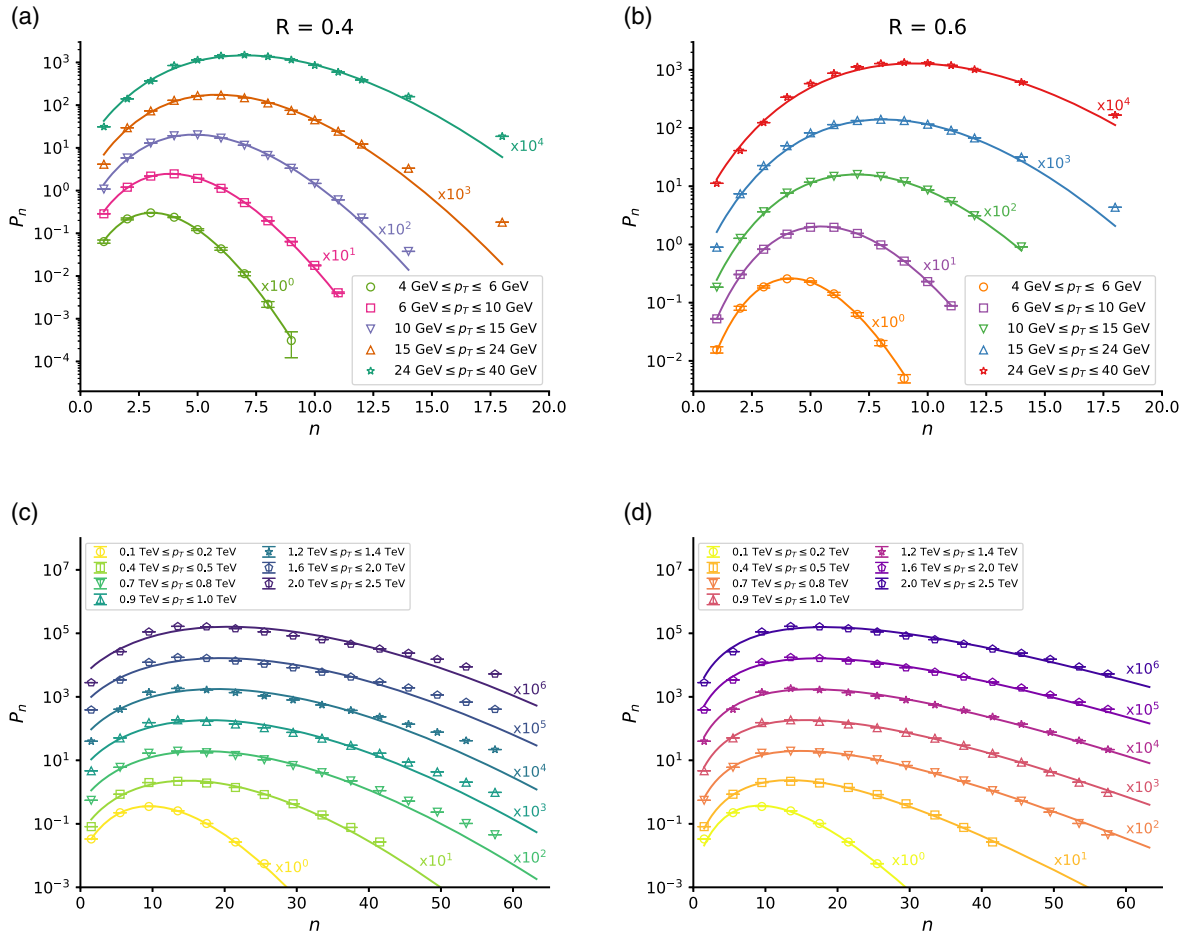

FIG. 4. Fits of the ATLAS data on jet multiplicity distributions for (a) $R = 0.4$ [15], (b) $R = 0.6$ [15], and data from Ref. [19] fitted with a (c) sub-Poisson distribution (14) and (d) with a negative binomial distribution (16).

TABLE II. Fitted α and δ from Eq. (14) for $R = 0.4$ and data from [15].

p_T range (GeV)	α	δ	χ^2
[4, 6]	12.8(2)	1.00(1)	0.06
[6, 10]	11.1(4)	0.64(2)	0.32
[10, 15]	10.2(5)	0.38(3)	1.36
[15, 24]	9.2(6)	0.20(4)	2.08
[24, 40]	7.2(5)	−0.02(4)	1.13

TABLE III. Fitted α and δ from Eq. (14) for $R = 0.6$ and data from [15].

p_T range (GeV)	α	δ	χ^2
[4, 6]	21.4(9)	0.98(3)	0.30
[6, 10]	15.7(3)	0.54(1)	0.06
[10, 15]	10.6(4)	0.17(2)	0.46
[15, 24]	8.5(6)	0.00(3)	1.55
[24, 40]	6.6(6)	−0.18(4)	1.32

distributions measured at higher energies are, as shown in [17,18], better described by NBD. This fact is interesting because it means a transition from one dynamical regime to another [29,30].

A detailed interpretation of these results in terms of the QCD dynamics is beyond the scope of this work but there are hints which may help theorists. We now present a few

TABLE IV. Fitted α and δ from Eq. (14), for ATLAS 2019 data [19].

p_T range (GeV)	α	δ
[100, 200]	3.13(6)	−0.505(8)
[400, 500]	2.30(9)	−0.69(1)
[700, 800]	2.0(1)	−0.74(2)
[900, 1000]	2.0(1)	−0.76(2)
[1200, 1400]	1.9(1)	−0.77(2)
[1600, 2000]	1.9(1)	−0.79(2)
[2000, 2500]	1.9(2)	−0.79(2)

TABLE V. Fitted $\bar{n}$ and k from Eq. (16), for ATLAS 2019 data [19].

p_T range (GeV)	$\bar{n}$	k
[100, 200]	10.5(1)	12(1)
[400, 500]	16.0(2)	7.4(4)
[700, 800]	18.5(2)	6.0(2)
[900, 1000]	19.6(2)	5.7(2)
[1200, 1400]	20.8(3)	5.4(3)
[1600, 2000]	22.0(4)	5.2(3)
[2000, 2500]	23.0(4)	5.2(3)

heuristic remarks, but further investigation is required for definite conclusions. They are the following:

(i) *Parton saturation*
The decreasing values of α suggest that the death rate must increase with the energy. In a parton cascade this would mean that the process $gg \to g$ becomes more important and when this happens we are approaching the gluon saturation regime. From Fig. 3 we see that the deviations from the standard perturbative QCD calculations occur at 1 TeV and this energy is high enough for saturation effects to become visible.

(ii) *Quark and gluon jets and phase space*
The initially positive values of δ render $P(n)$ narrow. This may be a consequence of phase space restrictions. At lower energies we have a smaller number of particles and energy-momentum conservation prevents large fluctuations. At higher energies and larger number of particles the fluctuations are also larger and $P(n)$ becomes broader. Alternatively, the narrowness of $P(n)$ at lower values of p_T may indicate that the jets are initiated by quarks. A broader $P(n)$ would indicate the dominance of gluon initiated jets.

(iii) *Threshold effects*
Based on the "parton liberation" picture [31] and on the "local parton-hadron duality" [32] we expect the $P(n)$ obtained from the parton cascade to be similar to the $P(n)$ of observed hadrons. In the parton model the average number of partons is related to the deep inelastic structure function and at high energies it is assumed that $\bar{n} \propto G(x, Q^2)$, where G is the gluon distribution. An increase in the number of gluons implies that the total momentum will be partitioned among more gluons and it becomes more likely to find a gluon with a small fraction of the total momentum. Particle production in the fusion of two gluons with momenta x_1 and x_2 introduces a threshold $x_1 x_2 \geq m^2/s$, where m is the (sum of the) mass(es) of the produced hadron(s) and $\sqrt{s}$ is the proton-proton collision energy. Imposing this restriction will exclude the lower x domain of $G(x)$ where the number of gluons grows rapidly and thus will exclude the larger n configurations. In other words, the imposition of particle production in a collision changes the solution of the parton cascade equation, favoring a narrower $P(n)$ with smaller $\bar{n}$. This motivates the use of the power index δ in the birth rate in Eqs. (5) and in (14). As the energy $\sqrt{s}$ increases the threshold constraint becomes less restrictive and allows for a larger number of gluons producing a larger number of final hadrons. As a consequence $P(n)$ becomes broader and with a larger $\bar{n}$. In Eq. (14) this behavior translates into a decreasing value of δ.

(iv) *Convolution, substructures and scaling*
In minimum bias proton-proton collisions typically half of the energy is released in the central rapidity region and the other half is carried by the remnants of the incoming protons. The fraction of the energy released in the central region may change with the energy [33]. This picture would suggest that the observed hadrons in the final state come from three sources. However the number of sources may be larger because the 'central fireball' may be composed of subsystems, smaller fireballs. This depends on details of the dynamics, i.e., perturbative or nonperturbative, with more or less string formation and decay, with or without thermalization, etc. In any case an important part of our understanding of the collision is to characterize the sources.

The number of sources will follow a distribution F and each source will emit a number of hadrons with a distribution G. Therefore the final multiplicity distribution P will be the result of the convolution $P = F \otimes G$. Alternatively, we can fix the number of sources to be one (which might be appropriate for jets) and let the average number of hadrons produced from this source, $\bar{n}$, to fluctuate according to a distribution F. Along this line, in Ref. [34] (see also [35]) it was shown that, P will follow KNO scaling (at large n and for finite $n/\bar{n}$) if it can be written as a convolution where G is a Poisson distribution and F a gamma function. In this case, the convolution $F \otimes G$ yielded a negative binomial distribution.

At lower energies, we do not observe scaling. On the other hand, at higher jet energies we observe empirically that KNO scaling is reached and also that the negative binomial distribution reproduces the data very well. This suggests that the limiting $P(n)$ for jets can be written as the convolution used in [34], allowing us to make conjectures about the fluctuations of $\bar{n}$ and about the nature of the sources.

V. CONCLUSIONS

In this work we have studied the multiplicity distribution of charged particles within jets in proton-proton collisions, which were measured by the ATLAS Collaboration. In the region $p_T < 500$ GeV the mean multiplicity as a function

of the jet transverse momentum is well-fitted by the QCD-NLLA and QCD-NMLLA formulas. At higher values of p_T these formulas overshoot the data. The low p_T data [15] do not show KNO scaling, whereas the higher p_T data [19] gradually approach KNO scaling. This is in line with the PYTHIA simulations presented in Ref. [17]. Using Eq. (14), which, depending on the sign of the δ parameter describes sub-Poissonian, Poissonian and super-Poissonian distributions, we have fitted all the existing data. However, at the highest values of p_T the best fit is obtained with the negative binomial distribution. The ratio $\bar{n}/k$ of the NBD fits is large, giving quantitative support to the approach to KNO scaling. The results presented here illustrate the research potential of the analysis of multiplicity distributions in high-energy jets for various values of transverse momenta p_T. As our analysis shows, different p_T ranges are described by different dynamics.

ACKNOWLEDGMENTS

We are grateful to the Brazilian funding agencies FAPESP, CNPq and CAPES and also to the INCT-FNA. G. W. was supported in part by the Polish Ministry of Education and Science, Grant No. 2022/WK/01.

[1] For a review see: W. Kittel and E. A. De Wolf, *Soft Multihadron Dynamics* (World Scientific, Singapore, 2005).
[2] J. F. Grosse-Oetringhaus and K. Reygers, J. Phys. G **37**, 083001 (2010).
[3] Z. Koba, H. B. Nielsen, and P. Olesen, Nucl. Phys. **B40**, 317 (1972).
[4] C. S. Lam and M. A. Walton, Phys. Lett. **140B**, 246 (1984).
[5] D. C. Hinz and C. S. Lam, Phys. Rev. D **33**, 3256 (1986).
[6] S. Hegyi, Nucl. Phys. B, Proc. Suppl. **92**, 122 (2001).
[7] A. Dumitru and Y. Nara, Phys. Rev. C **85**, 034907 (2012).
[8] A. Dumitru and E. Petreska, arXiv:1209.4105.
[9] Y. Liu, M. A. Nowak, and I. Zahed, Phys. Rev. D **108**, 034017 (2023); arXiv:2302.01380.
[10] V. Khachatryan *et al.* (CMS Collaboration), J. High Energy Phys. 01 (2011) 079.
[11] G. R. Germano and F. S. Navarra, Phys. Rev. D **105**, 014005 (2022); arXiv:2011.08912.
[12] Y. A. Kulchitsky and P. Tsiareshka, J. High Energy Phys. 10 (2023) 111; Eur. Phys. J. C **82**, 462 (2022).
[13] K. Ackerstaff *et al.* (OPAL Collaboration), Eur. Phys. J. C **1**, 479 (1998).
[14] H. W. Ang, M. Rybczyński, G. Wilk, and Z. Włodarczyk, Phys. Rev. D **105**, 054003 (2022).
[15] G. Aad *et al.* (ATLAS Collaboration), Phys. Rev. D **84**, 054001 (2011).
[16] Durham HepData Project, https://www.hepdata.net/record/57743?.
[17] R. Vértesi, A. Gémes, and G. G. Barnaföldi, Phys. Rev. D **103**, L051503 (2021).
[18] Z. Varga and R. Vértesi, Symmetry **14**, 1379 (2022).
[19] G. Aad *et al.* (ATLAS Collaboration), Phys. Rev. D **100**, 052011 (2019).
[20] G. Aad *et al.* (ATLAS Collaboration), Eur. Phys. J. C **76**, 322 (2016).
[21] A. H. Mueller, Phys. Lett. **104B**, 161 (1981).
[22] B. R. Webber, Phys. Lett. **143B**, 501 (1984).
[23] E. D. Malaza, Phys. Lett. **149B**, 501 (1984); E. D. Malaza and B. R. Webber, Nucl. Phys. **B267**, 702 (1986).
[24] I. M. Dremin and R. C. Hwa, Phys. Lett. B **324**, 477 (1994).
[25] I. M. Dremin and J. W. Gary, Phys. Rep. **349**, 301 (2001).
[26] R. Perez-Ramos and D. d'Enterria, J. High Energy Phys. 08 (2014) 068.
[27] R. Medves, A. Soto-Ontoso, and G. Soyez, J. High Energy Phys. 10 (2022) 156.
[28] P. Abreu *et al.* (DELPHI Collaboration), Phys. Lett. B **416**, 233 (1998).
[29] C. C. Shih, Phys. Rev. D **34**, 2720 (1986).
[30] P. Carruthers and C. C. Shih, Int. J. Mod. Phys. A **02**, 1447 (1987).
[31] A. H. Mueller, Nucl. Phys. **B572**, 227 (2000).
[32] Y. L. Dokshitzer, V. A. Khoze, S. I. Troian, and A. H. Muller, Rev. Mod. Phys. **60**, 373 (1988).
[33] G. N. Fowler, F. S. Navarra, M. Plumer, A. Vourdas, R. M. Weiner, and G. Wilk, Phys. Rev. C **40**, 1219 (1989).
[34] M. Praszalowicz, Phys. Lett. B **704**, 566 (2011); A. Bialas, Acta Phys. Pol. B **41**, 2163 (2010).
[35] S. Mrówczyński, Z. Phys. C **27**, 131 (1985).